Eur. Phys. J. B **52**, 83–90 (2006)
DOI: 10.1140/epjb/e2006-00266-x

THE EUROPEAN PHYSICAL JOURNAL B

Driven lattice gas with nearest-neighbor exclusion: shear-like drive

F.Q. Potiguar[a] and R. Dickman[b]

Departamento de Física, ICEx, Universidade Federal de Minas Gerais, 30123-970, Belo Horizonte, Minas Gerais, Brazil

Received 3 October 2005 / Received in final form 27 March 2006
Published online 6 July 2006 – © EDP Sciences, Società Italiana di Fisica, Springer-Verlag 2006

Abstract. We study the lattice gas with nearest-neighbor exclusion on the square lattice and Kawasaki (hopping) dynamics, under the influence of a nonuniform drive, via Monte Carlo simulation. The drive, which favors motion along the $+x$ direction and inhibits motion in the opposite direction, varies linearly with y. (The boundaries along the drive direction are periodic, so that the system is not described by an equilibrium Gibbs distribution.) As in the uniformly driven case [R. Dickman, Phys. Rev. E **64**, 16124 (2001)], the onset of sublattice ordering occurs at a lower density than in equilibrium, but here an unexpected feature appears: particles migrate out of the high-drive region. For intermediate system sizes ($L \simeq 100$), the accumulation of particles is sufficient for the low-drive region to become ordered at a global density of about 0.3. Above this density we observe a surprising reversal in the density profile, with particles accumulating to the high-drive region, due to jamming. For larger systems ($L \geq 200$) particles quickly jam in the high-drive region, as occurs under uniform drive, and the accumulation of particles in the low-field region is severely reduced.

PACS. 05.10.Ln Monte Carlo methods – 05.70.Ln Nonequilibrium and irreversible thermodynamics – 64.60.Ht Dynamic critical phenomena

1 Introduction

The lattice gas is a basic model system of interacting particles with excluded volume, and has been used extensively to study equilibrium properties of simple fluids. Nonequilibrium versions have also been widely studied [1,2], generally via the imposition of a "drive" that biases hopping along one of the principal axes of the lattice [3]. Lattice gases with biased hopping are also known as *driven diffusive systems* (DDS) [1]; the repulsive version [4,5] serves as a model for fast ionic conductors [6]. The stationary properties of driven, nonequilibrium lattice gases depend strongly on the kind of dynamics and on the manner in which the bias is implemented, unlike in equilibrium, where the energy function and boundary conditions are the sole determining factors. The phase diagram and critical behavior of DDS has attracted much interest in recent years [1,2].

The lattice gas with nearest-neighbor exclusion (NNE) is the infinite-repulsion limit of the lattice gas with nearest-neighbor repulsion. In this limit particles are forbidden to occupy the same or neighboring sites; the minimum allowed interparticle separation is that of second neighbors. Hard-core exclusion is the only interaction between the particles, so the model is a minimal lattice version of the hard-sphere fluid. (This model also represents the zero-neighbor limit of the Biroli-Mézard lattice glass model [7].) The equilibrium version was studied in [8–13] both theoretically and numerically, for various lattice types. These analyses show that the model exhibits a continuous phase transition to an ordered state at a critical density ρ_c ($\approx$0.367 on the square lattice), with exponents that belong to the Ising universality class [13]. This order-disorder transition occurs in bipartite lattices, i.e., those that may be decomposed into two sublattices, A and B, such that the nearest-neighbors of any sites in sublattice A belong to sublattice B and vice-versa. The equilibrium version also models hard core bosons [14].

More recently, driven versions of the NNE model were studied [15,16]. In reference [15] it was found, for the case of nearest-neighbor hopping dynamics on the square lattice, that the critical density decreases with increasing bias. The transition is continuous for weak bias but becomes discontinuous under sufficiently strong drive. In the latter case, above the transition density, the system separates into regions of low and high local density, with the high-density region essentially frozen or *jammed*; sublattice ordering is observed only in the jammed region. Szolnoki and Szabó [16] extended the dynamics to include next-nearest-neighbor (diagonal) hopping, and observed a similar variation of the critical density with drive strength, but with a uniform particle distribution. Continuous phase

[a] e-mail: potiguar@fisica.ufmg.br
[b] e-mail: dickman@fisica.ufmg.br

transitions in this version of the model fall in the Ising class, as in equilibrium [16]. These results suggest that there are two ordering scenarios in the driven NNE lattice gas: one (continuous) that depends on unequal sublattice occupancies to accomodade high particle densities, as in equilibrium, and a second in which a discontinuous transition is provoked by the formation of a jammed region.

As part of the ongoing effort to characterize the phases of driven systems [1,2], and motivated by the surprising redistribution of particles observed in the NNE model under uniform drive, we study here the effects of a *nonuniform* drive. We present results of Monte Carlo (MC) simulations of a NNE lattice gas in which the drive varies linearly with position, imitating the velocity profile of a sheared fluid. Our main objective is to obtain the phase diagram of the model. We determine the critical density and study the behavior of the order parameter and the stationary current as functions of density in systems of $L \times L$ sites, with L ranging from 20 to 500. This type of driving field was used in a study of cluster aggregation in a simple lattice model without nearest-neighbor exclusion [17].

Of particular interest is how the particles are distributed under the nonuniform drive, as reflected in the density, current and order parameter profiles. We find that at intermediate sizes ($L \approx 100$), at global densities lower than about 0.33, particles tend to accumulate in the low-drive region. Surprisingly, this tendency is sufficiently strong for the density in this region to exceed the transition density of the equilibrium system. Thus, as the global density is increased, ordering first occurs in the low-drive region. This is quite different from the uniform-drive case, in which a *large* bias facilitates ordering. Moreover, this represents a new mechanism for the phase transition in the driven NNE model, as the ordering is not accompanied by jamming. As the global density is increased beyond 0.30, the tendency for particles to accumulate in the low-drive region is gradually reversed. The high-drive region becomes denser, leading to the jamming phenomenon observed in reference [15]. For system sizes $L \geq 200$, the accumulation of particles in the low drive is weaker than in smaller lattices. This is because the high-drive region jams at a lower global density, closer to the value found under uniform drive.

Numerical studies of phase transitions normally probe the large-system limit, by applying finite-size scaling (FSS) analysis to results for various system sizes. In the present case such an analysis is hindered by the fact that, if we maintain one side of the system at zero drive, and the other at maximum, then the gradient ($\propto 1/\mathrm{L}$) weakens with increasing system size, and for large L the behavior may approach that of a uniformly driven system. If, on the other hand, one fixes the magnitude of the drive gradient at $1/L_{max}$, one may study various system sizes ($\leq L_{max}$) at *fixed gradient*. But now one has various choices for the range of drive values, in systems with $L < L_{max}$. In summary, there is no way to study a sequence of "equivalent" systems of different size as required for FSS analysis. We do consider two examples of systems with different sizes but the same field gradient, and show how the order parameter and current change with different maximum and minimum fields.

The balance of this paper is organized as follows. We detail the model and simulation procedure in Section 2. In Section 3 present numerical results and analysis, and discuss the mechanism behind the nonuniform density profile. We summarize our results in Section 4.

2 Simulations

We study a system of N particles on a square lattice of $L \times L$ sites. The NNE condition implies that if site (i, j) is occupied, the four neighboring sites, $(i \pm 1, j)$ and $(i, j \pm 1)$, must be vacant. Naturally, two particles may not occupy the same site. Thus the particle density $\rho = N/L^2 \leq 1/2$. The dynamics is via local hopping. At each attempted move, a particle is selected at random and assigned a new (trial) position at one of the nearest neighbor sites, with probabilities as discussed below. If the trial position does not violate the exclusion constraint, the move is accepted, otherwise it is rejected. The initial configuration is prepared via random sequential adsorption (RSA) [18,19] of particles, always respecting the excluded-volume condition. Once all N particles have been inserted, the hopping dynamics begins. We define a time unit as N attempted moves, and generally follow the evolution for 10^6 time units.

The drive is imposed by biasing the probabilities for hopping along the x-direction; the system has periodic boundaries in this direction. In the direction perpendicular to the drive we impose reflecting boundaries: moves to $y = 0$ or $y = L+1$ are prohibited. The bias is defined in terms of the probability P_r for a particle to attempt a jump to the right ($x \to x + 1$); the probability for attempting to hop to the left is $P_l(y) = 1/2 - P_r(y)$, and $1/4$ in the $+y$ and $-y$ directions. Thus $P_r = 1/4$ in equilibrium (zero bias) while $P_r = 1/2$ corresponds to maximum bias (hopping in the $-x$-direction prohibited). We study linear bias profiles, with $P_r(y)$ varying from a certain minimum $p_{min} \geq 1/4$ at $y = 1$, to a maximum, $p_{max} \leq 1/2$, at $y = L$. The drive gradient magnitude is defined as $\kappa \equiv 4(p_{max} - p_{min})/(L - 1)$. The simplest case is:

$$P_r(y) = \frac{1}{4}\left(1 + \frac{y-1}{L-1}\right), \tag{1}$$

i.e., no bias at $y = 1$, maximum bias at $y = L$, and gradient $\kappa = 1/(L - 1)$.

3 Results

3.1 Stationary global properties

To begin, we consider the drive profile of equation (1). We treat the global particle density ρ as the control parameter, in systems of size $L = 20$, 50, 100, 200 and 500. To obtain a preliminary notion of the phase diagram, we study the order parameter and the stationary current. The

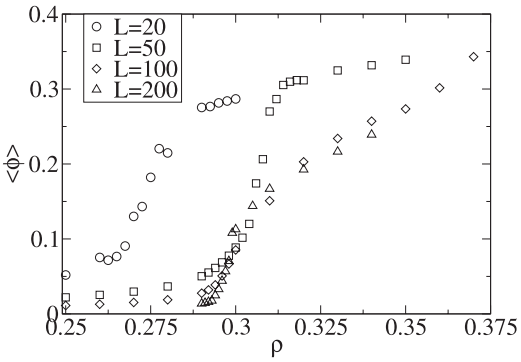

Fig. 1. Order parameter vs. global density.

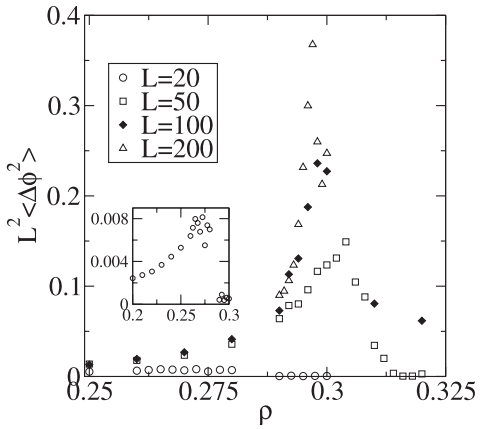

Fig. 2. Scaled variance of the order parameter vs. global density.

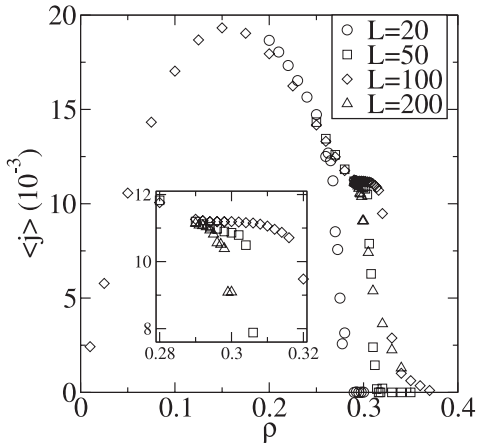

Fig. 3. Stationary current density versus global density.

order parameter is defined as the difference in sublattice occupancies per site,

$$\langle \phi \rangle = \frac{\langle |N_A - N_B| \rangle}{L^2}, \qquad (2)$$

where N_A (N_B) is the number of particles in sublattice $A(B)$ and $\langle\,\rangle$ indicates a stationary time average, as well as an average over independent realizations (we use the same notation for all other quantities). Note that complete ordering corresponds to $\langle \phi \rangle = \rho$. We performed 100, 50 and 25 independent realizations for $L = 20, 50$, $L = 100$ and $L = 200$, respectively.

Figure 1 shows the global order parameter (i.e., averaged over the entire system) as a function of global density ρ, in the stationary state. The rapid rise in the order parameter suggests that the system undergoes a phase transition near $\rho = 0.29$. The transition appears to be continuous, motivating the study of the scaled variance of the order parameter, $\chi = L^2 \langle (\Delta\phi)^2 \rangle$, where $\Delta\phi = \phi - \langle \phi \rangle$, (Fig. 2). (In equilibrium, χ represents the staggered susceptibility per site, and diverges at ρ_c in the infinite-size limit. The results for $L = 200$ represent averages over 50 independent realizations in this case.)

The maximum in χ grows with system size, suggesting that it diverges as $L \to \infty$, as expected for a continuous phase transition. We estimate the transition density as $\rho_c = 0.297(1)$. The critical density is clearly lower than in equilibrium, $\rho_c \approx 0.367$ [9,13].

In the *uniformly* driven system [15], the transition (for maximum bias and $L = 100$) occurs at a density of 0.272, and is *discontinuous*. It is interesting to note that in the uniform case, a transition density of $\rho_c = 0.30$ is obtained for $P_r = 3/8$; under these conditions the transition is discontinuous. The transition in the uniformly driven system is continuous for $P_r \leq 0.3$. In fact, the value of the drive in the ordered region of the system studied here satisfies this inequality. Of note in Figure 2 is the anomalously small value for $L = 20$. This is due to the fact that for this small system size, most realizations become frozen on the time scale of the simulations, as is also reflected in the current (Fig. 3).

The current density is defined as the difference between the number of jumps along the drive and the number contrary to it, per site and unit time. This quantity (Fig. 3) displays a similar behavior as in the uniformly driven case: it increases at small densities (reflecting the increasing number of carriers) and decreases for larger densities (due to the reduction in available space for movement). The maximum value of $\langle j(t) \rangle$ falls at roughly in the same density as in the uniform drive case [15]. For $L = 100$ we observe a plateau in $\langle j \rangle$ (see inset of Fig. 3). Following the plateau the current decreases precipitously. The plateau is not seen for $L = 50$ or $L = 200$. (In the latter case the current decreases rapidly in the critical region.) In Section 3.2 below we will give a qualitative explanation of these results based on the density and current profiles.

The order parameter and the stationary current exhibit strong fluctuations at densities above $\rho = 0.32$. The evolution of these quantities typically displays sudden jumps between the ordered and the disordered state, a fact already observed in the uniformly driven case [15]. The drive provokes formation of organized structures while thermal motion provides a mechanism for their break-up. The strong fluctuations, and slow relaxation, render it difficult to obtain precise results for the order parameter and current in this regime. Typically, to obtain reliable results, we have to increase the simulation time by a factor of 10.

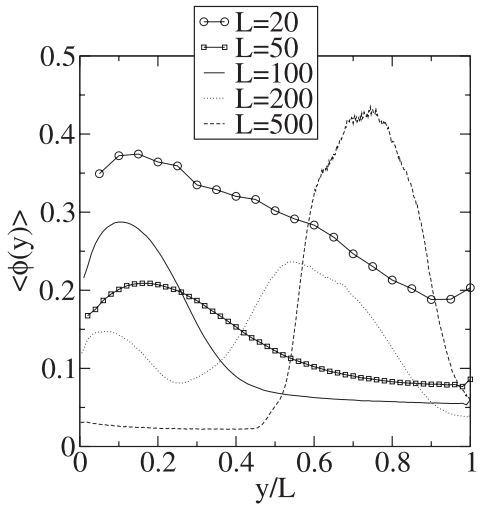

Fig. 4. Order parameter profiles for global density of 0.30.

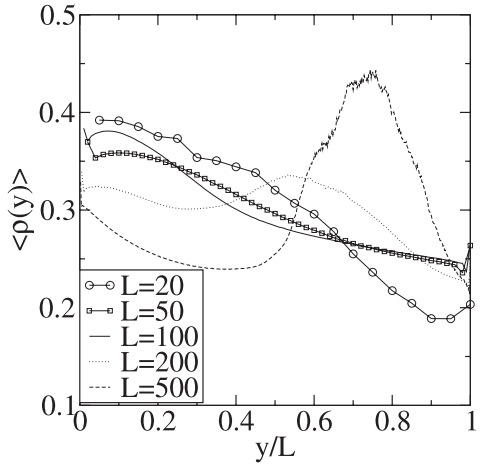

Fig. 5. Density profiles for a global density value of 0.30.

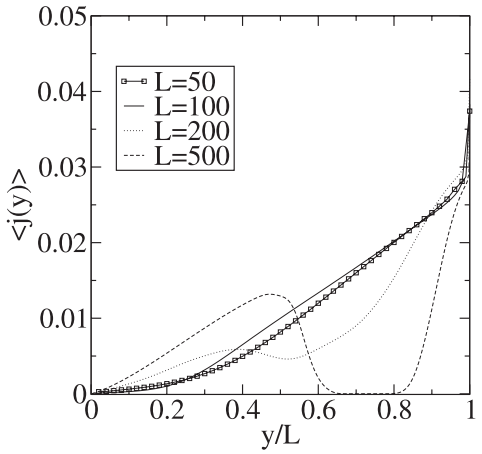

Fig. 6. Current profiles for $\rho = 0.30$. For $L = 20$ the current is extremely small.

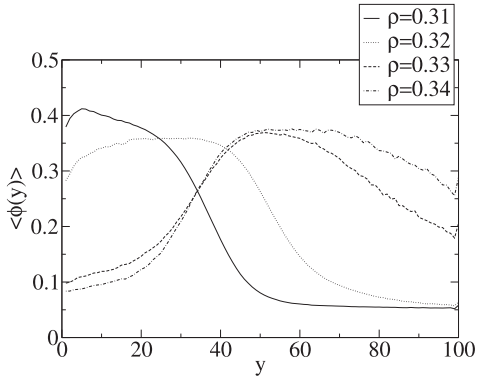

Fig. 7. Order parameter profile for global densities as indicated, $L = 100$.

3.2 Profiles

To better understand how the system organizes, we analyze the order parameter, density and current profiles, $\langle\phi(y)\rangle$, $\langle\rho(y)\rangle$ and $\langle j(y)\rangle$, respectively. They are defined exactly as their global counterparts, except that they are normalized by the number of sites in a line, L, instead of the total number of sites. These quantities are shown in Figures 4–6 for a global density of 0.30.

These density profiles show that for $L \leq 100$, particles are expelled from the high-drive region. (The case of $L = 20$, as noted above, is anomalous). For larger system sizes the picture is quite different: the expulsion of particles is no longer evident at density $\rho = 0.30$, although it does occur at slightly smaller densities. We instead observe (for $\rho = 0.30$), a marked accumulation in a region closer to that of maximum drive. In both cases, the high-density region is more ordered than the rest of the system as seen in Figure 4. For $L \geq 200$, the accumulation of particles in the low drive region is less pronounced than for $L < 200$, and is not associated with a transition to an ordered phase.

Particle accumulation appears to be the mechanism behind the phase transition (see Fig. 2) and the change in the variation of the current with density. From the order parameter profiles, it is evident that ordering is restricted to the regions with higher density. As we increase the global density, particles accumulate in specific regions, and the global order parameter increases continuously.

The current profiles indicate that the current is predominantly in the high-drive region. Since for $L = 100$ most of the particles accumulate in the low-drive region, the overall value of the stationary current is barely affected by a change in the global density close to the critical point, leading to the observed plateau in Figure 3. The situation is different for $L \geq 200$ because most of the particles jam in the high-drive region, leading to a sharp drop in the global current just above the transition.

We show the profiles for $L = 100$ at higher global densities (up to $\rho = 0.34$), in Figures 7–9. Enhanced particle concentration in the low-drive region is in fact observed for densities as low as $\rho = 0.20$, for this system size. For global density $\rho \simeq 0.32$, the density profile $\rho(y)$ (Fig. 8) is highly skewed to the region around $y = 0$, where the bias is small. Note that the local density is ≥ 0.37 in this region (for ρ between 0.30 and 0.32), that is, greater than or equal to ρ_c in equilibrium. The density profile decays

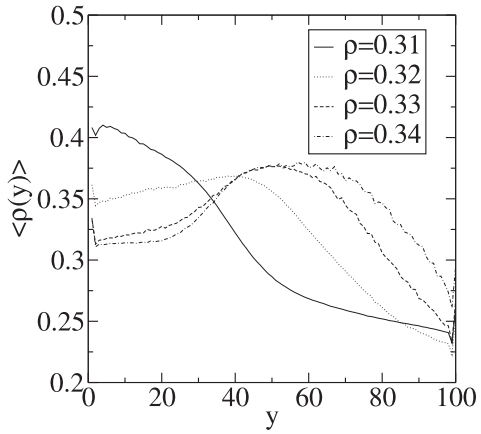

Fig. 8. Density profile for a global densities as indicated, $L = 100$.

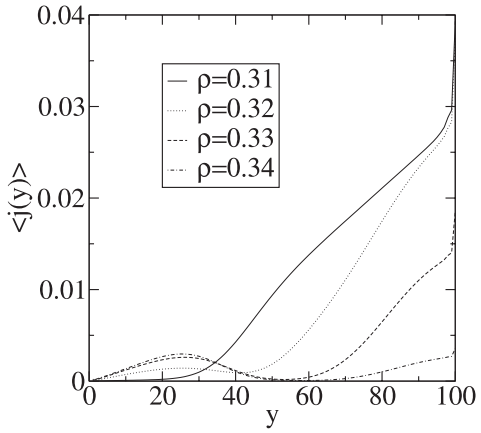

Fig. 9. Current profile for global densities as indicated, $L = 100$.

monotonically with increasing y (except for small density oscillations induced by the wall at $y = 0$).

For higher global densities the tendency reverses. At a global density of $\rho = 0.33$, the local density *increases* with y, reaching a peak near $y = 47$, after which it decays in an approximately linear fashion. For a certain range of global densities, the local density near $y = 1$ actually *decreases* with increasing ρ. Turning to the current profiles (Fig. 9), we see that as the global density is increased, the current rapidly decreases (as is already evident from Fig. 3), and progressively shifts to the low-drive region. Results for $\rho > 0.35$ (not shown here) indicate that the current in the high-drive region is essentially zero for this range of densities.

3.3 Ordering and jamming

The surprising reversal of the density and current profiles with increasing global density is related to the formation of a jammed region, as observed in the uniformly driven system [15]. A jammed region is one in which all movement is blocked (except for motions of particles trapped in cages); the diffusion constant and mobility are zero in such regions. When the global density is too low for a jammed region to form, particles tend to collect in the low-drive region because a strong drive tends to destroy the local correlations needed for particles to pack to high density. When, on the other hand, the global density is sufficiently high for a jammed region to form, it appears in the high-drive region, leading to an irreversible accumulation of particles there, so that the low-drive region has fewer particles than at lower global densities.

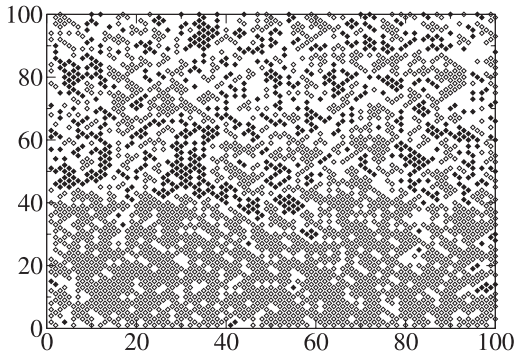

Fig. 10. Particle configuration at density $\rho = 0.31$, after 10^6 MC steps (system size $L = 100$). Open and filled symbols represent particles in different sublattices. The drive is directed to the right and increases in the vertical direction.

To illustrate these ideas, we show in Figure 10 a configuration for $\rho = 0.31$ and $L = 100$ (all the results in this subsection are for this system size). As expected, the low-drive region is very dense and contains few mobile particles. In the uniformly driven system (at maximum bias) one observes, at this density, formation of a "herringbone" pattern of diagonal stripes, pointing along the drive, with particles in this structure essentially frozen (this is closer to the form of the jammed region for $L \geq 200$). In the present case the low-drive region is highly ordered, with almost all particles in the same sublattice, but there is no sign of the herringbone pattern. The high-drive region is disordered, permitting the high currents and lower densities reported above. Several clusters are seen in the high-drive region, but they are not large enough to cause jamming.

For global densities above about 0.34, the situation, as noted, is completely changed. Particles now accumulate in the high-drive region, and the density profile exhibits a maximum in the central region (intermediate drive strength). At these higher densities the current profile displays a peak in the low-drive region. The peak shifts to smaller y (smaller bias) and decreases in amplitude as the global density is increased.

Figure 11 shows a typical configuration at global density $\rho = 0.35$. Evidently the long diagonal line of particles at the upper right is associated with jamming in the high-drive region. The empty triangular region implies a decrease in the local density with increasing y. Particles are not free to enter this region since all particles along the diagonal edge are jammed. These observations are supported by the density and current profiles (Figs. 5 and 6). The density is roughly constant in the middle portion of

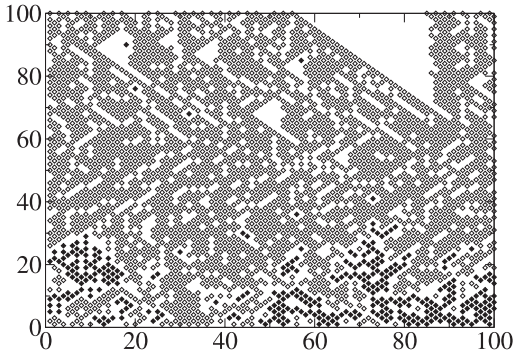

Fig. 11. Particle configuration at density $\rho = 0.35$, after 10^6 time units ($L = 100$).

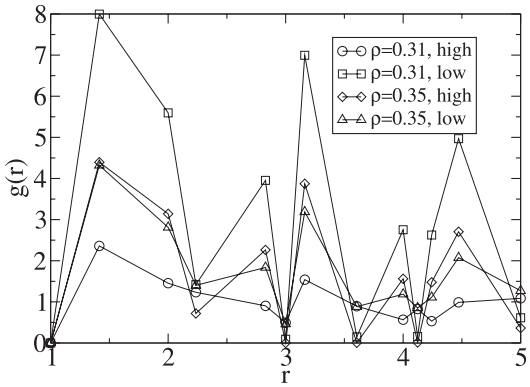

Fig. 12. Radial distribution function for the high- and low-drive regions, for densities $\rho = 0.31$ and $\rho = 0.35$. The error bars are the same size or smaller than the symbols.

the lattice and begins to decrease near $y = 78$, where the empty triangular region begins. The current is only appreciably different from zero in the lower portion of the lattice, as signalled in Figure 11 by the presence of particles in both sublattices. The diagonal edges observed in configurations at this density (always in the high-drive region), are extremely long-lived structures, since only the particle at the tip of the line can move without violating the exclusion constraint. Even these particles are able to move only rarely, so that this structure does not change on the time scale of the simulation.

To study interparticle correlations, we determine the radial distribution function, $g(r)$ in the high- and low-drive regions (Fig. 12). This function is proportional to the probability of finding a pair of particles separated by a distance r, and is normalized so that $g \to 1$ as $r \to \infty$. For purposes of determining $g(r)$, the low-drive region is taken as the strip $6 \leq y \leq 14$, while the high-drive region comprises $86 \leq y \leq 94$.

The $g(r)$ curves for global density $\rho = 0.31$ show that the high- and low-drive structures are markedly different. In the low-bias region the peaks are much larger due to sublattice ordering associated with packing of particles, and are compatible with long-range order (LRO). The high-drive region shows little structure; the oscillations in $g(r)$ decay rapidly with distance. Again, the picture for $\rho = 0.35$ is quite different. The sharpness of the peaks

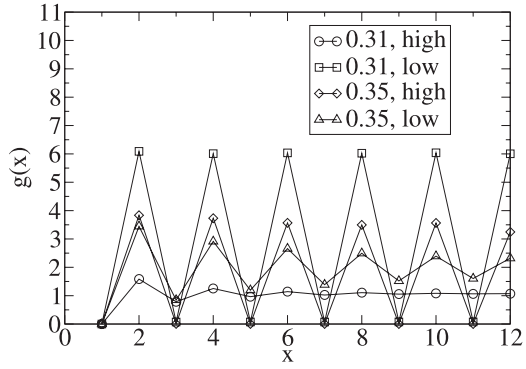

Fig. 13. Pair correlation function (unnormalized) along the drive direction for the high- and low-drive regions, for densities $\rho = 0.31$ and $\rho = 0.35$. The error bars are the same size or smaller than the symbols.

in $g(r)$ in the high-bias region, for $\rho = 0.35$, reflects the very different sublattice densities, as does the fact that $g \simeq 0$ for $r = 3$, $\sqrt{13}$ and $\sqrt{17}$. The radial distribution function in the low-drive region, for this density, exhibits less structure, consistent with the more equal sublattice occupancies.

In Figure 13 we show the joint probability (unnormalized) for a pair of sites, separated by a distance x along the drive direction, to be simultaneously occupied. (Here, low- and high-drive regions are those for $y \leq 50$ and $y > 50$, respectively.) This figure makes clear the existence of LRO in the low-drive region at global density 0.31, and the complete absence of such order in the high-drive region. For a global density of 0.35, LRO is evident in the high-drive region due to the formation of jammed structures, as described above. It is unclear whether LRO persists in the low-drive region.

Figure 14 shows the joint probability (again unnormalized) for simultaneous occupation of a pair of sites separated by a distance y, *perpendicular* to the drive. We measured this quantity in two sections of the lattice: $12 < y \leq 38$ and $62 < y \leq 88$, corresponding to low and high drive. For global density 0.31 correlations along y have practically the same structure as those along x, although the amplitude of $g(y)$ is slightly smaller than $g(x)$. For $\rho = 0.35$, the high-bias region possesses a nearly isotropic LRO. At this density the low-bias region exhibits anisotropic correlations, with $g(x)$ decaying more rapidly than $g(y)$.

3.4 Results for fixed drive gradient and varying system size

In this subsection we consider the results for the global order parameter and stationary current for different system sizes but with the same drive gradient κ. We first consider a gradient of $\kappa \approx 0.01$, for $L = 100$ and $L = 50$. In the latter case, the bias varies between zero and half its maximum value (case $50-I$), from half-maximum to maximum (case $50-II$), and from a quarter to three-quarters of the

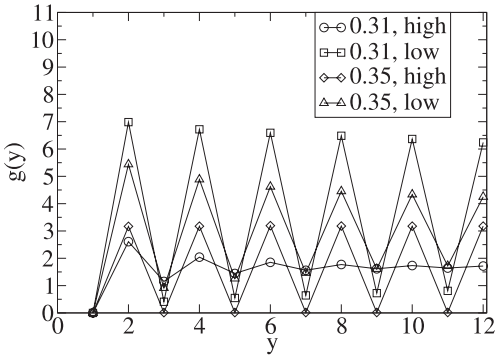

Fig. 14. Pair correlation function (unnormalized) perpendicular to the drive direction measured in regions of low and high bias, for densities $\rho = 0.31$ and $\rho = 0.35$. The error bars are the same size or smaller than the symbols.

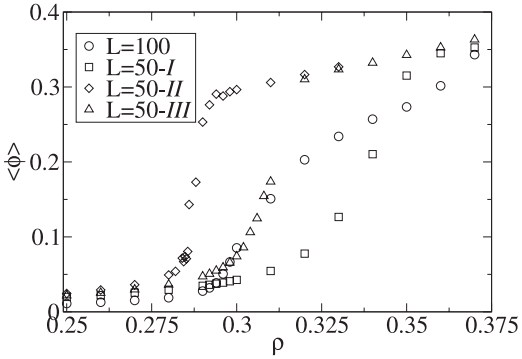

Fig. 15. Order parameter for $L = 100$ and the three $L = 50$ systems with the same drive gradient, $\kappa \approx 0.01$.

maximum (case $50 - III$). Figures 15 and 16 show both results.

In case $50 - II$ the variation of the order parameter suggests a discontinuous transition around $\rho = 0.282(2)$. Correspondingly, the stationary current drops sharply at this density. For cases $50 - I$ and $50 - III$, the variation of the order parameter and current with global density is much smoother, with no sign of discontinuities, even though the derivative $\partial\langle\phi\rangle/\partial\rho$ is clearly larger for $50 - III$ than for $50 - I$. It is interesting to note that the critical densities in the three smaller lattices are different; the smallest value is for $50 - II$. The next largest is for case $50 - III$, which is very close to the critical density of the $L = 100$ case, while the largest critical density is found in case $50 - I$.

For a bias gradient of $\kappa \approx 0.005$, we studied system sizes $L = 200$ and $L = 100$. There are now two cases for $L = 100$, analogous to cases $50 - I$ and $50 - II$, termed $100 - I$ and $100 - II$. Figures 17 and 18 show the results for the order parameter and the stationary current, respectively.

These two plots strengthen the conclusions drawn earlier: for $100 - II$ the order parameter curve has the features of a discontinuous transition, around $\rho = 0.2755$, while the results for $100 - I$ shows a clearly continuous transition. Again, the critical densities of the smaller systems are different and have the same pattern as those for the cases before: $\rho_c(100 - I) < \rho_c(100 - II)$.

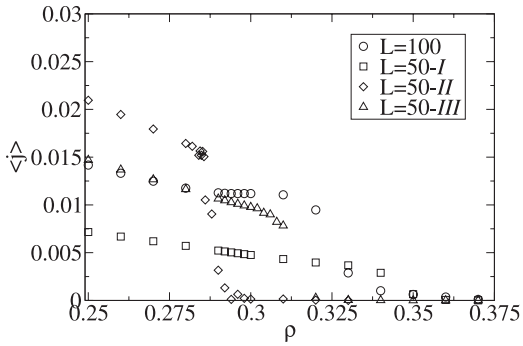

Fig. 16. Current density for the same cases as in Figure 15.

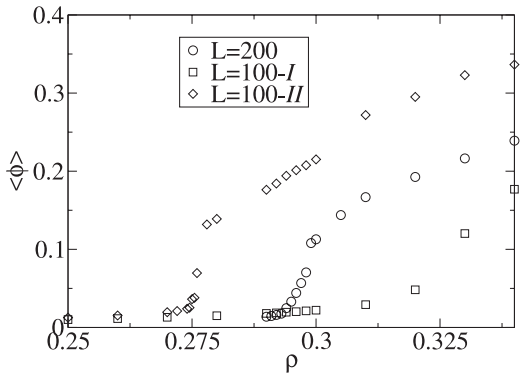

Fig. 17. Order parameter for $L = 200$ and the two $L = 100$ cases, all with the same drive gradient, $\kappa \approx 0.005$.

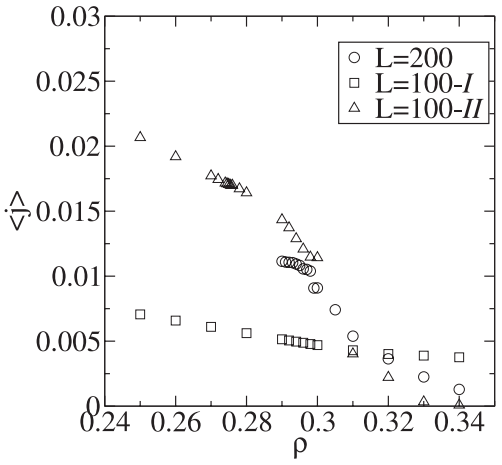

Fig. 18. Current density for the same states as those in Figure 17.

A glance at the average probability $\overline{P}_r = \frac{1}{L}\sum_{y=1}^{L} P_r(y)$, for a jump in the $+x$ direction helps to understand the above results for the critical densities and the nature of the transitions. Its value for the drive profile of equation (1) is 0.375. In cases I, II and III the values are 0.3125, 0.4375 and 0.375, respectively, regardless of the system size L. Since the critical density decreases with bias, we should expect the critical densities in cases I,

II and *III* to be lower, higher and equal to the full gradient case.

For large systems in which the bias profile varies from zero to maximum, both tendencies, accumulation of particles in the low-drive region, and jamming in that of high drive, are present. For example, a system with $L = 500$ exhibits, at a global density of 0.25, enhanced concentration of particles in both high- and low-bias regions. The result of the complementary tendencies is a continuous transition, as can be inferred from Figure 1.

4 Conclusions

We study a lattice gas with nearest-neighbor exclusion driven by a nonuniform, shear-like drive, on the square lattice, under nearest-neighbor hopping dynamics. The problem is of interest both as an example of the surprising behavior to be found in a simple nonequilibrium system, and as a toy model for a granular or colloidal system under shear. We find that the system with a drive profile of equation (1) (no bias at one wall, maximum at the other) undergoes a continuous order-disorder transition at a critical density of about $\rho_c = 0.297(1)$. This is unlike the uniformly driven model, in which the transition is discontinuous for a bias $\geq$0.75. Despite the fact that, in this series of studies, the drive gradient decreases as we increase system size, we see no evidence of a change to a discontinuous transition for large L. In particular, the data for the variance of the order parameter, $\langle(\Delta\phi)^2\rangle$, (Fig. 2) suggest the transition remains continuous as $L \to \infty$.

Our results show that in this case order-disorder transition is due to the concentration of particles in definite portions of the lattice. For $L \leq 100$, the phenomenon occurs at low-bias region, for global densities between $\rho = 0.28$ and 0.32. Remarkably, the nonuniform drive induces a highly nonuniform density profile, expelling particles from the high-bias region. The effect is sufficiently strong to induce sublattice ordering in the low-bias region. Thus the drive favors a class of configurations that, on the basis of entropy maximization, would be extremely unlikely in equilibrium. Note that at these densities there is no jamming, i.e., the system is ergodic. Migration of particles to the low-bias region appears to derive from the destruction of short-range correlations, required for efficient packing, by the drive. For higher densities, we observe a completely inverted picture, with formation of jammed structures in the high-drive region, while particles outside this region remain mobile. The jammed region is characterized by a dense ($\rho \geq 0.37$) strip of particles; at higher global densities this region displays long diagonal chains of particles associated with voids. Preliminary studies show that the concentration effects also appear if half the system has *no bias* while the remainder is subject to maximum bias [20].

The situation for larger lattices ($L \geq 200$) is different. The accumulation occurs simultaneously in two regions, in the vicinity of the walls. This reflects the fact that for increasing system size, the field gradient, $\kappa \approx 1/L$, leading to a behaviour similar to that of the uniformly driven system, in different parts of the lattice. In the high-bias region, the field quickly induces particle aggregation, while particles slowly accumulate in the low-bias region as well. We expect that the infinite size limit, the transition is continuous, with ordering occuring first near the walls, and spreading to the rest of the lattice with increasing global density.

It is natural to ask how the system studied here may be studied theoretically. At the microscopic level, solution of the full master equation seems impossible, but various truncations or *cluster mean-field theories* have been devised for driven systems [1,2]. In models with nearest-neighbor exclusion, however, one must use rather large clusters (consisting of six or more sites), to observe any effect of the drive, as shown by Szolnoky and Szabó [16]. A possible approach would be a spatially inhomogeneous version of the six-site approximation, involving 17 variables at each position, along the direction perpendicular to the drive. Another possibility is a coarse-grained description in terms of the particle and order-parameter densities, along the lines of a time-dependent Ginzburg-Landau theory. To construct such a theory one would need to develop plausible expressions for the dependence of the parameters (such as the excluded volume interaction, for example) on the drive. We defer investigation of these approaches to future work.

We thank the Brazilian agencies CAPES, CNPq and Fapemig for support.

References

1. B. Schmittmann, R.K.P. Zia, *Statistical Mechanics of Driven Diffusive Systems*, Vol. 17, *Phase Transitions and Critical Phenomena* (Academic Press, London, 1995)
2. J. Marro, R. Dickman, *Nonequilibrium phase transitions in lattice models* (Cambridge University Press, Cambridge, 1999)
3. S. Katz, J. Lebowitz, H. Spohn, Phys. Rev. B **28**, 1655 (1983)
4. K.-T. Leung, B. Schmittmann, R.K.P. Zia, Phys. Rev. Lett. **62**, 1772 (1989)
5. R. Dickman, Phys. Rev. A **41**, 2192 (1990)
6. J.B. Boyce, B.A. Huberman, Phys. Rep. **51**, 189 (1979)
7. G. Biroli, M. Mézard, Phys. Rev. Lett. **88**, 25501 (2002)
8. D.S. Gaunt, M.E. Fisher, J. Chem. Phys. **43**, 2840 (1965)
9. F.H. Ree, D.A. Chesnut, J. Chem. Phys. **45**, 3983 (1966)
10. L.K. Runnels, L.L. Combs, J. Chem. Phys. **45**, 2482 (1966)
11. D.S. Gaunt, M.E. Fisher, J. Chem. Phys. **46**, 3237 (1967)
12. R.J. Baxter, I.G. Enting, S.K. Tsang, J. Stat. Phys. **22**, 465 (1980)
13. W. Guo, H.W.J. Blöte, Phys. Rev. E **66**, 46140 (2002)
14. N.G. Zhang, C.L. Henley, Phys. Rev. B **68**, 14506 (2003)
15. R. Dickman, Phys. Rev. E **64**, 16124 (2001)
16. A. Szolnoky, G. Szabó, Phys. Rev. E **65**, 47101 (2002)
17. O.J. O'Loan, M.R. Evans, M.E. Cates, Physica A **258**, 109 (1998)
18. P. Meakin, J.L. Cardy, E. Loh, D.J. Scalapino, J. Chem. Phys. **86**, 2380 (1987)
19. R. Dickman, J.-S. Wang, I. Jensen, J. Chem. Phys. **94**, 8252 (1991)
20. F.Q. Potiguar, R. Dickman, in preparation (2006)